

Article

# Microstructures and Mechanical Properties of Mg-9Al/Ti Metallurgical Bonding Prepared by Liquid-Solid Diffusion Couples

Jiahong Dai <sup>1,2</sup>, Bin Jiang <sup>2,3,\*</sup>, Qiong Yan <sup>1</sup>, Hongmei Xie <sup>1</sup>, Zhongtao Jiang <sup>4</sup>, Qingshan Yang <sup>5</sup>, Qiaowang Chen <sup>4</sup>, Cheng Peng <sup>1,\*</sup> and Fusheng Pan <sup>2,3</sup>

<sup>1</sup> College of Materials Science and Engineering, Yangtze Normal University, Chongqing 408100, China; jiahongdai@foxmail.com (J.D.); yanqiong@163.com (Q.Y.); xiehongmei@yznu.cn (H.X.)

<sup>2</sup> State Key Laboratory of Mechanical Transmissions, College of Materials Science and Engineering, Chongqing University, Chongqing 400044, China; fspan@cqu.edu.cn

<sup>3</sup> Chongqing Academy of Science and Technology, Chongqing 401123, China

<sup>4</sup> Research Institute for New Materials Technology, Chongqing University of Arts and Sciences, Chongqing 402160, China; jiangtao6364@163.com (Z.J.); chenqiaowang1999@163.com (Q.C.)

<sup>5</sup> School of Metallurgy and Materials Engineering, Chongqing University of Science and Technology, Chongqing, 401331, China; qsyang@cqu.edu.cn

\* Correspondence: jiangbinrong@cqu.edu.cn (B.J.); 20090008@yznu.cn (C.P.); Tel.: +86-135-9419-0166 (B.J.); +86-136-5826-7036 (C.P.); Fax: +86-0236-5111-140 (B.J.); +86-0237-2790-029 (C.P.)

Received: 23 August 2018; Accepted: 28 September 2018; Published: 29 September 2018



**Abstract:** Microstructures and mechanical properties of Mg-9Al/Ti metallurgical bonding prepared by liquid-solid diffusion couples were investigated. The results indicate that a metallurgical bonding was formed at the interface Mg-9Al/Ti, and the Mg<sub>17</sub>Al<sub>12</sub> phase growth coarsening at the interfaces with the increase in heat treatment time. Push-out testing was used to investigate the shear strength of the Mg-9Al/Ti metallurgical bonding. It is shown that the shear strength presents an increasing tendency with the increased heat treatment time. The sequence is characterized, and the results show that the fracture takes place along the Mg-9Al matrix at the interface. The diffusion of Al and Ti elements play a dominant role in the interface reaction of Mg-9Al/Ti metallurgical bonding. By energy-dispersive spectroscopy (EDS), X-ray diffraction (XRD) and thermodynamic analysis, it was found that Al<sub>3</sub>Ti is the only intermetallic compound at the interface of Mg-9Al/Ti metallurgical bonding. These results clearly show that chemical interaction at the interface formation of Al<sub>3</sub>Ti improves the mechanical properties of Mg-9Al/Ti metallurgical bonding.

**Keywords:** magnesium; titanium; metallurgical bonding; interface; mechanical properties

## 1. Introduction

Magnesium alloys, as the lightest metal structural materials, have high specific strength, excellent castability, and easy recyclability. However, the application of commercially available Mg alloys is limited to applications because of their lower strength [1–3]. Titanium alloys have been widely used due to their high specific strength, notable impact toughness, excellent corrosion resistance and significant thermal stability [4]. However, the high production cost restricts their widespread applications [5]. Bimetal materials have been widely used in many industrial fields because they combine several promising properties that cannot be provided by monolithic materials. Mg and Ti bimetal materials have drawn great attention due to its unique properties, which can combine low density of magnesium and extraordinarily high specific strength and significant thermal stability of Ti [6].

In the past several years, it has been reported that Al/Mg, Mg/Mg and Al/Ti bimetal materials have already been fabricated by accumulative roll-bonding [7], extrusion forming [8], laser welding–brazing [9], and so forth. However, these methods still have much room for improvement as their processing procedures are very complex and the products usually have lower interface bonding strength and little opportunity for mass production. In recent years, the liquid-solid casting process method has been also utilized to produce Al/Mg [10], Mg/Mg [11] and Al/Ti [12] bimetal materials, which exhibits excellent industrial application prospects for the preparation of bimetallic materials due to the low production costs, simple production procedure and high interface bonding strength of the products. However, so far, Mg/Ti bimetal materials prepared by the liquid-solid casting process method have not been reported yet.

Obtaining a perfect metallurgical bonding in the interface between Mg and Ti is very important to guarantee the excellent mechanical properties for the Mg/Ti bimetallic materials. However, Mg and Ti are not phase formation. Furthermore, the solid solution between Mg and Ti is very low [13]. These indicate that no interfacial reaction or atomic diffusion occurs between Mg and Ti. Hence, an intermediate element must be added to react with Mg and Ti or solid solubility in Mg and Ti. Al is the dominant alloying element to improve the mechanical properties of Mg alloys and Ti alloys, which can form intermetallic compounds during solidification due to the reaction of Al with Mg or Ti. The hybrid structure of (Mg-Al)-Ti dissimilar metal by welding has been investigated by the welding-brazing method [14–16]. Brazing interfaces were composed of intermetallic compound  $Ti_3Al$ , which was resistance to the crack propagation and improvement of mechanical properties. Therefore, a perfect metallurgical bond can be formed at the interface between Mg-Al alloy and Ti by the liquid-solid casting process, but the formation of Mg-Al alloy and Ti metallurgical bonding has not been declared yet.

Based on this condition, Mg-9Al alloy and Ti were studied in this paper to produce excellent metallurgical bonding by the liquid-solid diffusion couples. The microstructure and mechanical behaviors at the interface of Mg-9Al/Ti metallurgical bonding are further discussed.

## 2. Experiments

Mg-9Al (Mg-9 wt.%Al) casting ingots and Ti rods with dimensions of  $\Phi 8 \text{ mm} \times 100 \text{ mm}$  were used. The surface of Ti rods was polished with 1000-grit SiC papers before application and subsequently treated with acetone cleaning. Then, Mg-9Al ingots were put in a stainless-steel crucible with  $\Phi 34 \text{ mm} \times 90 \text{ mm}$  (showed in Figure 1), which was kept in a resistance furnace under a protective atmosphere of  $CO_2 + 0.5 \text{ vol.}\% SF_6$ . Mg-9Al alloy was held at  $700 \text{ }^\circ\text{C}$  for melting. After melting, Ti rod was rapidly submerged into the molten Mg-9Al alloy. A steel cover was set on top of the crucible when the insert experiment was carried out so that the Ti rod would be kept vertical and centered (shown in Figure 1). Next, the liquid-solid diffusion couples of Mg-9Al/Ti were formed. Diffusion couples were kept at  $700 \text{ }^\circ\text{C}$  for 0 min, 30 min and 60 min. After that, diffusion couples were furnace cooled to room temperature.

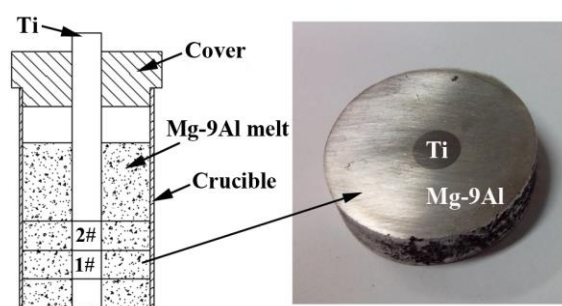


**Figure 1.** The schematic sketch of preparing Mg-9Al/Ti metallurgical bonding prepared by liquid-solid diffusion couples.

The samples were cut from the middle part of the diffusion couples perpendicular to the rod axis with a thickness of 9 mm. Each sample was ground with ground papers from 400 to 1000 grit to cross-sectional scanning electron microscopy (SEM, TESCAN VEGA 3 LMH, TESCAN Co., Brno, Czech) examinations. SEM equipped with energy-dispersive spectroscopy (EDS) (Oxford Instrument Technology Co., Ltd., Oxford, UK) was employed to determine the concentration profiles of the interfaces and phase composition of the interface. Additionally, the phase structure for the fractured specimen of the interface was determined by X-ray diffraction (XRD, D/Max 2500PC, Dandong Fangyuan Instrument Co., Ltd., Dandong, China).

The shear strength of the metallurgical bonding interface was investigated by push-out testing (NEW SANSEI CMT-5105, XinSanSi (Shanghai) Enterprise Development Co., Ltd., Shanghai, China). The schematic diagram is illustrated in Figure 2. The supporting platform is a diameter of a centered circular hole of 10 mm. The diameter of the steel cylinder was 6 mm. The loading rate of cross-head was 1 mm/min. Shear strength of the metallurgical bonding interfaces was calculated by the following equation:

$$\tau = \frac{F_{\max}}{2\pi r t} \quad (1)$$

where  $F_{\max}$  is the maximum load,  $r$  is the radius of Ti insert, and  $t$  is the specimen thickness.

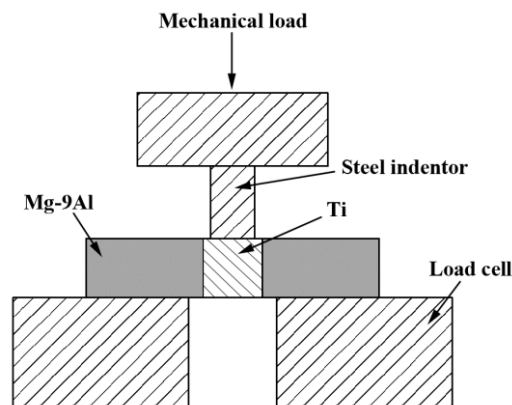
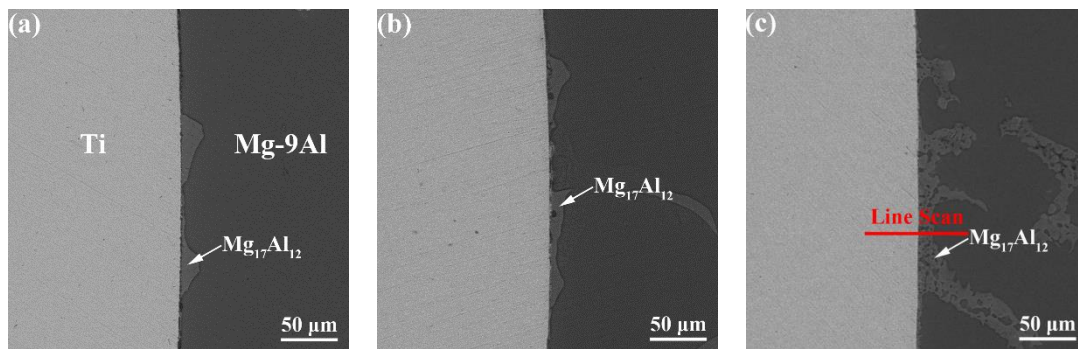


Figure 2. A schematic diagram of the push-out tests.

### 3. Results and Discussion

#### 3.1. The Microstructure of the Interface

Cross-sectional backscattered electron (BSE, TESCAN Co., Brno, Czech) micrographs at the interface of Mg-9Al/Ti metallurgical bonding prepared by the liquid-solid diffusion couples at different heat treatment times are presented in Figure 3. It can be noted that the  $Mg_{17}Al_{12}$  phase in the Mg-9Al matrices are attached to the surface of Ti rods. The  $Mg_{17}Al_{12}$  phases growth coarsened with the increase of heat treatment time at the interfaces. The  $Mg_{17}Al_{12}$  phases are distributed along the grain boundaries of Mg-based matrix. They increased with increasing temperature, and the grain boundaries wetting transitioned from incompletely wetted to completely wetted by the  $Mg_{17}Al_{12}$  phase. Because the contact angle between Ti and  $Mg_{17}Al_{12}$  phase decreases with increasing temperature [17], and the reversible grain boundary (GB) transitioned from incomplete to complete, wetting by a liquid phase always proceeds with increasing temperature. This is due to the temperature dependence  $2\sigma_{SL}(T)$  always being more steep than the dependence  $\sigma_{GB}(T)$ , as the liquid phase possess higher entropy in comparison to the solid one [18]. Figure 3a shows a cross-sectional BSE micrograph image at the interface of Mg-9Al/Ti at 700 °C for 0 min. Obviously, a gap was established at the interface between Mg-9Al alloy and Ti rod. In addition, the cross-sectional BSE micrograph images at the interface of Mg-9Al/Ti at 700 °C for 30 min and 60 min are indicated in Figure 3b,c. The specimens formed a complete metallurgical bonding at the Mg-9Al/Ti interface.



**Figure 3.** Cross-sectional backscattered electron (BSE) micrographs of interfaces between Mg-9Al matrix and Ti rod obtained at 700 °C for (a) 0 min, (b) 30 min, (c) 60 min.

Figure 4a shows a magnified image of the interface between Mg-9Al matrix and Ti after 60 min at 700 °C. The intermetallic compounds have developed around the Ti rod at the interface that can be observed. The composition of point A was analyzed by EDS in Figure 4b. The EDS result is taken from the testing position A denoted in Figure 4a. The composition of Al is 57.12 at.% and Ti is 39.45 at.% for point A. The ratio of Al/Ti is 3.06. It can be inferred that the intermetallic compound is  $\text{Al}_3\text{Ti}$ . This is in agreement with the reports of Jie et al. [19] and Li et al. [20] that formation of  $\text{Al}_3\text{Ti}$  between liquid Al and solid Ti, but the results are inconsistent with Cao et al. [14] and Tan et al. [15,16] studies. Therefore, further proof is needed. As can be seen in Figure 4a, there are a large number of nanostructures at the interface. It is reported in the literature that these nanostructures will accelerate the diffusion of adatoms and improve the wettability of the interface [21–23].

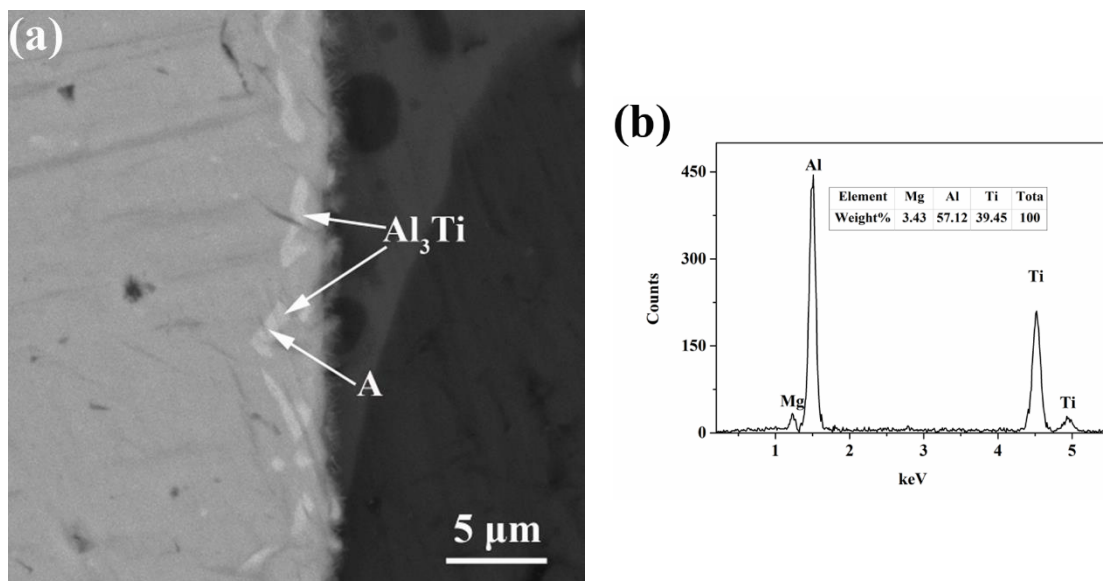


**Figure 4.** (a) The high magnification image of the interface between Mg-9Al matrix and Ti rod obtained after 60 min at 700 °C, (b) Energy-dispersive spectroscopy (EDS) result of the point A.

The interface of Mg-9Al matrix and Ti rod obtained after 60 min at 700 °C was analyzed using EDS through line scan in Figure 5. At the interface between Mg-9Al matrix and Ti rod, the element Ti tends to decrease at the interface when approaching Mg-9Al matrix. The concentration of Ti in  $\text{Mg}_{17}\text{Al}_{12}$  phase is obviously higher than that of Mg matrix. Moreover, at the interface between Mg-9Al matrix and Ti rod, the elements of Mg and Al vary clearly, indicating the decreasing tendency when approaching Ti side. Therefore, it can be inferred that the diffusion of Al and Ti elements may play an

important role during the interface of Mg-9Al/Ti metallurgical bonding. Moreover, because of the interdiffusion between Al and Ti, the  $\text{Al}_3\text{Ti}$  compound is formed at the interface.

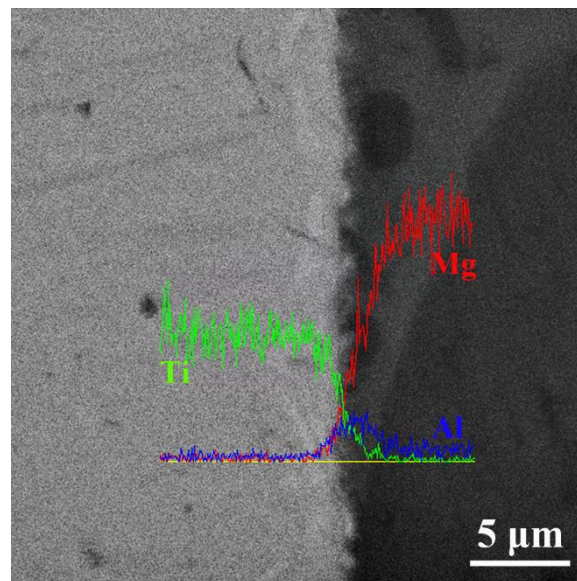


**Figure 5.** Line scan curves of the interface between Mg-9Al matrix and Ti rod obtained after 60 min at 700 °C.

The concentration profiles of the interface between Mg-9Al matrix and Ti rod annealed after 60 min at 700 °C showed in Figure 6 which are line scan results in Figure 3c. The trend of element distribution is consistent with the results of Figure 5. According to Hall's method [24], the impurity diffusion coefficients of Mg in Ti and Al in Ti, and Ti in Mg-9Al. The results are  $1.70(\pm 0.02) \times 10^{-15} \text{ m}^2/\text{s}$ ,  $3.77(\pm 0.12) \times 10^{-15} \text{ m}^2/\text{s}$ ,  $1.60(\pm 0.23) \times 10^{-14} \text{ m}^2/\text{s}$ , respectively. It can be seen that the diffusion of Al in Ti is faster than the Mg in Ti. Ti diffuse in Mg-9Al is faster than Al and Mg impurity diffusion in Ti, which may be related to the state of Ti and Mg-9Al alloy. So the diffusion of Al and Ti elements play an important role during the interface of Mg-9Al/Ti metallurgical bonding.

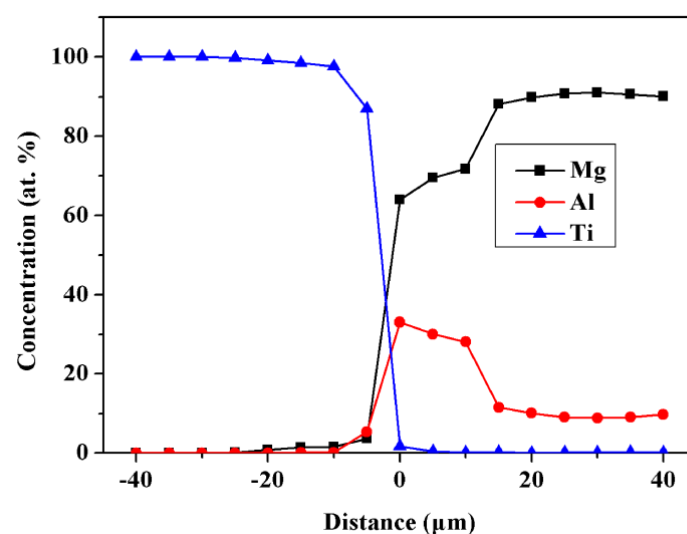


**Figure 6.** Concentration profiles of the interface between Mg-9Al matrix and Ti rod annealed after 60 min at 700 °C.

### 3.2. Mechanical Behaviors

Figure 7 shows the load-displacement curves. It is noticeable that the shear strength of Mg-9Al/Ti metallurgical bonding presents an increasing tendency for the extension of the heat treatment time. The average shear stress at the interface can be evaluated by Equation (1). Results of shear strength for Mg-9Al/Ti metallurgical bonding under different heat treatment time are listed in Table 1. It can be seen that the shear strength of the Mg-9Al/Ti metallurgical bonding with the increase of heat treatment time in this study, and the maximum value is 56 MPa.

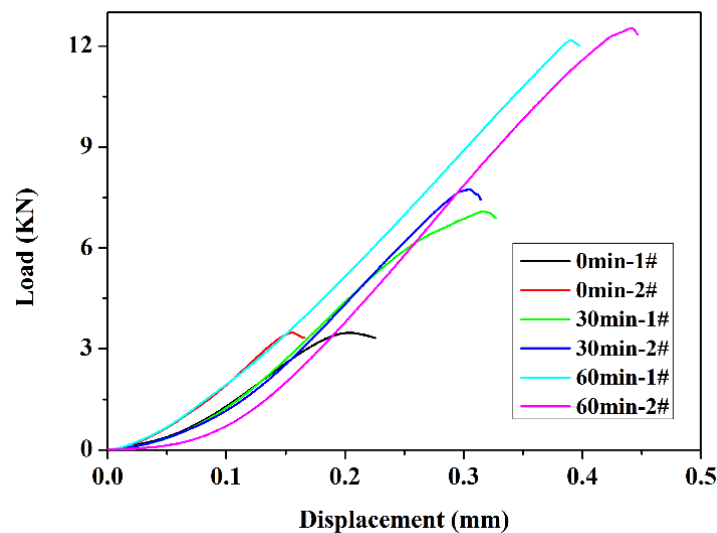
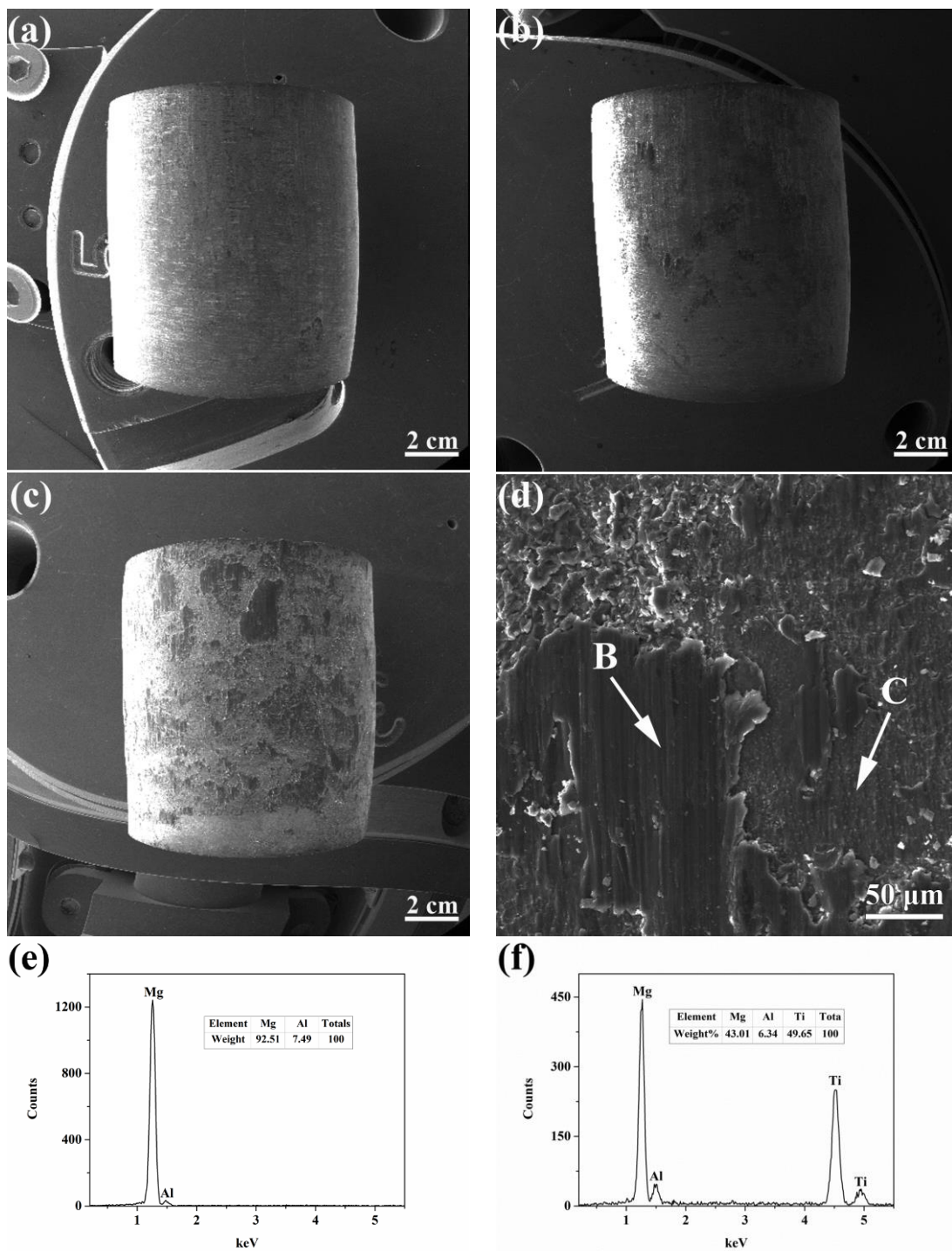


**Figure 7.** Load-displacement curves obtained of the Mg-9Al/Ti metallurgical bonding by push-out testing for 0 min, 30 min and 60 min at 700 °C.

**Table 1.** Shear strength of Mg-9Al/Ti metallurgical bonding with different heat treatment time.

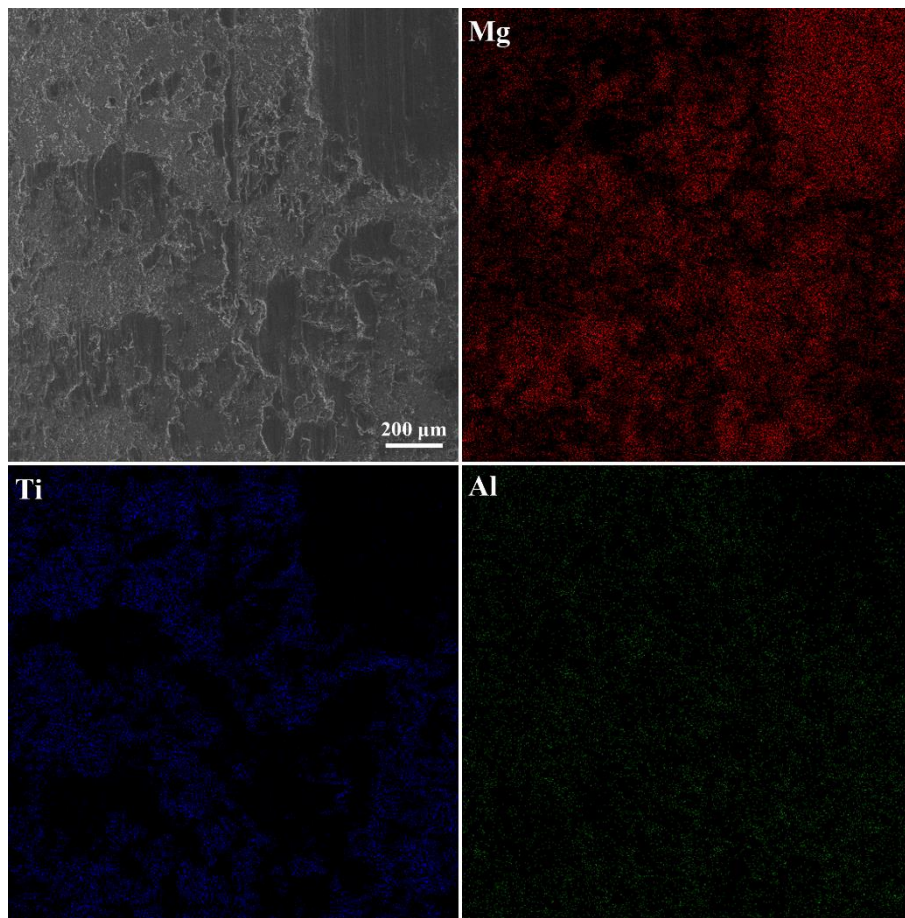
Sample	Maximum Stress (N)	Maximum Shear Strength (MPa)
0 min-1#	3478	16
0 min-2#	3482	16
30 min-1#	7086	32
30 min-2#	7742	35
60 min-1#	12,174	54
60 min-2#	12,531	56

Figure 8a–c shows SEM fractographs on the Ti insert of the Mg-9Al/Ti metallurgical bonding push-out samples obtained by different heat treatment time. It can be seen that the surface roughness of the Ti rod face increase with the increase of heat treatment time. Figure 8d shows the magnified image of the fracture surface of Ti side at 700 °C for 60 min. The fracture is characterized by long grooves, all with the same orientation parallel to the push-out direction, characteristic of a ductile fracture. Figure 8e–f shows EDS analyses of the point B and C in Figure 7d. So the point B is Mg-9Al matrix, the point C is the interface of Mg-9Al/Ti metallurgical bonding. Figure 9 shows the distribution of Mg, Al and Ti elements for the fracture surface of Ti side at 700 °C for 60 min. It is observed that the Al element in Mg-9Al matrix diffuses into the Ti rod. Those are indicating that the shear stress has been greatly improved when Al and Ti interdiffuse and chemical interaction occurs between Mg-9Al and Ti, and grain boundaries between Ti and Mg-9Al wetting transition from incompletely wetted to completely wetted by Mg<sub>17</sub>Al<sub>12</sub> phase. So Mg-9Al/Ti metallurgical bonding becomes firm and impervious with heat treatment time.



**Figure 8.** BSE fractographs of Ti rod for (a) 0 min, (b) 30 min, (c) 60 min; (d) magnified image of the Ti rod for 60 min; (e) EDS of the point B; (f) EDS of the point C.

To understand the mechanism of crack formation and propagation during shear strength tests, it is necessary to identify where the crack initiation occurs. Figure 10 illustrates the cross-sectional BSE image of the Mg-9Al/Ti metallurgical bonding interface for 60 min. It can be found that the fracture takes place along the Mg-9Al matrix of the interface.



**Figure 9.** BSE-EDS mapping of Mg, Al and Ti elements for the fracture surface of Ti rod at 700 °C for 60 min.

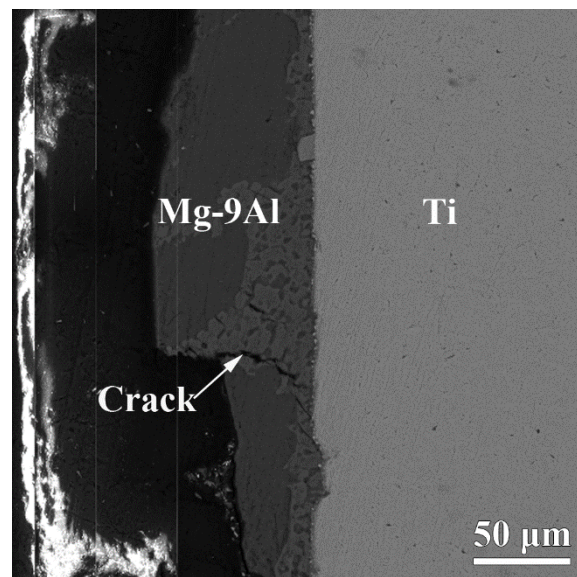


**Figure 10.** BSE cross-sectional view of the Mg-9Al/Ti metallurgical bonding at 700 °C for 60 min.

To characterize the intermetallic compounds formed at the interface of the Mg-9Al/Ti metallurgical bonding, X-ray diffraction was carried out for the Mg-9Al/Ti metallurgical bonding fractured surfaces for heat treatment at 700 °C for 60 min. The XRD patterns are shown in Figure 11.

According to the XRD patterns, Mg, Ti,  $Mg_{17}Al_{12}$  and  $Al_3Ti$  on both fractured surfaces of the Mg-9Al and Ti fractured surface. However, Mg and  $Mg_{17}Al_{12}$  patterns of the Ti fracture surfaces were higher than the Ti patterns at the Mg-9Al fracture surfaces. The result showed that the fracture path is propagated through the Mg-9Al matrix.  $Al_3Ti$  were formed via the reaction of Al and Ti at the interface. This is in agreement with the EDS results of the interface between Mg-9Al and Ti matrices obtained after 60 min at 700 °C.

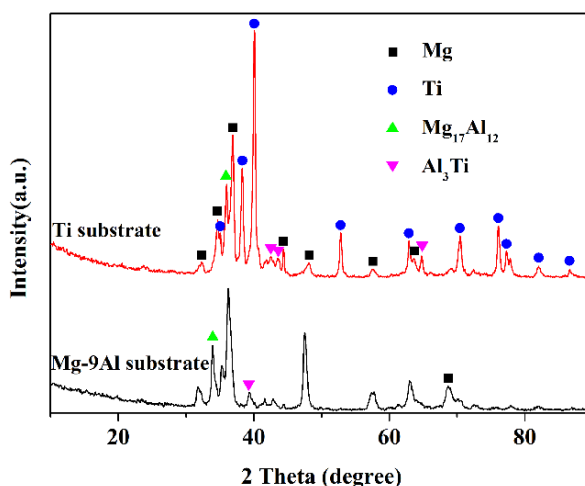


**Figure 11.** X-ray diffraction patterns from the fractured specimen at 700 °C for 60 min.

### 3.3. Thermodynamic Analysis of Intermetallic Compounds Formation at the Interface

From Mg-Ti binary phase diagram, Mg and Ti hardly forms a chemical reaction. However, the Al-Ti binary phase diagram is shown in Figure 12. It can be seen that several intermetallic compounds, namely, AlTi,  $Al_2Ti$ ,  $Al_5Ti_2$ ,  $Al_3Ti$  and  $AlTi_3$ . Therefore, Mg-Al and Al-Ti intermetallic compounds are likely to form in the interface of Mg-9Al/Ti metallurgical bonding. The thermodynamics is an important factor in determining whether an intermetallic compound can be formed. The Miedema's model for the enthalpy of formation is used to calculate the standard molar enthalpies of formation of Mg-Ti, Mg-Al and Al-Ti binary systems [9,16]. These calculations indicate that the standard molar enthalpy of Mg-Ti binary system was positive, but Al-Mg and Al-Ti binary systems were negative. The standard molar enthalpy of Al-Ti binary system was more negative than that of Al-Mg binary system, which indicates that Al-Ti intermetallic compound prefers to be formed at the interface of the Mg-9Al/Ti in the same condition.

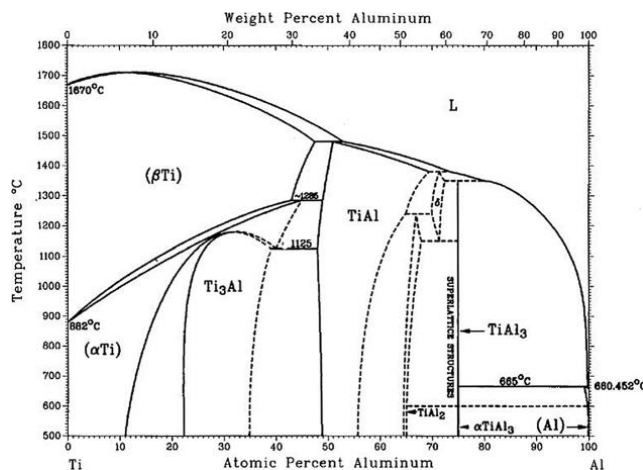


**Figure 12.** Al-Ti binary phase diagram.

Previous studies involving the synthesis of titanium aluminides through powder metallurgical routes showed that  $\text{Al}_3\text{Ti}$  forms prior to the formation of any other titanium aluminides belonging to the binary Ti–Al system [25]. Formation of  $\text{Al}_3\text{Ti}$  has also been reported during the interaction between solid Ti and liquid Al [26]. However, the reason was not evaluated clearly. The possible reason for the preference can be explained by considering the thermodynamic drive force at the Mg–Al/Ti interface. This is based on the temperature dependence of Gibbs free energy of formation of various Al–Ti compounds from the literature [27,28]. In previous studies, the sublattice model (Wagner–Schottky model) was used to calculate Gibbs free energies of formation of  $\text{AlTi}_3$ ,  $\text{AlTi}$ ,  $\text{Al}_3\text{Ti}$ ,  $\text{Al}_2\text{Ti}$  and  $\text{Al}_5\text{Ti}_2$ . The final expressions obtained for Gibbs free energies of formation for the compounds are presented in Table 2. The values of Gibbs free energies are calculated in the temperature range of 373–1073 K and the results obtained are shown in Figure 13. It can be found in this figure that in this temperature range, the Gibbs free energy of the  $\text{Al}_3\text{Ti}$  is lower than the  $\text{AlTi}$  and  $\text{AlTi}_3$ , and is higher than the  $\text{Al}_2\text{Ti}$  and  $\text{Al}_5\text{Ti}_2$ , but the  $\text{Al}_2\text{Ti}$  and  $\text{Al}_5\text{Ti}_2$  must react with  $\text{AlTi}$  through a series of reactions. So  $\text{Al}_3\text{Ti}$  is expected to be the first phase to form in the Al–Ti system. This is in agreement with the EDS and XRD results of the interface between Mg–9Al and Ti obtained at 700 °C after 60 min. However, there was only a small number of Al diffusion to the Ti rod in this study, so the formation of  $\text{Al}_3\text{Ti}$  compound was less.

**Table 2.** Temperature dependence of Gibbs free energy of formation of various Ti–Al compounds, data from ref. [21].

Compound	Free Energy of Formation, $\Delta G$
$\text{AlTi}_3$	$-9,633.6 + 6.70801T$
$\text{AlTi}$	$-37,445.1 + 16.79376T$
$\text{Al}_3\text{Ti}$	$-40,349.6 + 10.36525T$
$\text{Al}_2\text{Ti}$	$-43,858.4 + 11.02077T$
$\text{Al}_5\text{Ti}_2$	$-40,495.4 + 9.52964T$

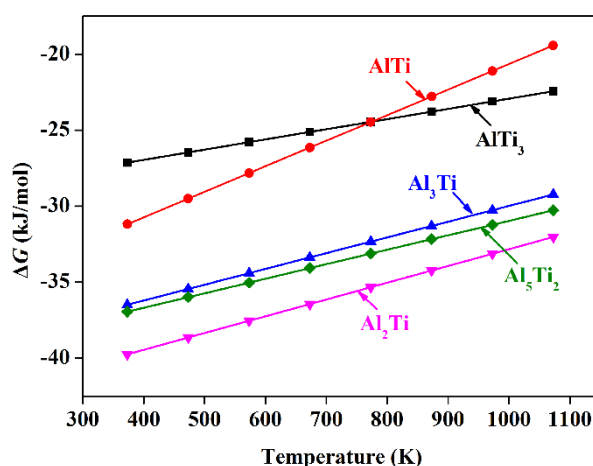


**Figure 13.** Gibbs energy of formation,  $\Delta G$ , of different compounds as a function of temperature.

### 3.4. The Metallurgical Reaction Mechanism of the Solid/Liquid Interface

Metallurgical reaction mechanism of Mg–9Al/Ti interface by liquid–solid diffusion couples was clarified with the schematic diagram shown in Figure 14. Under the experimental temperature, the Ti rods were rapidly submerged into the molten Mg–9Al alloy. Mg and Ti did not react with each other. However, Al and Ti can be the formation of several Al–Ti intermetallic compounds. The Al atoms diffuse from the molten Mg–9Al alloy filler to the liquid/solid interface and Ti substrate. Al atoms were mixed with Ti atoms for the Ti substrate and diffusing from Ti substrate at the liquid/solid interface, indicated in Figure 14a,b. Tan et al. [16] found that for the same Ti content, the chemical potential of Al decreased as the Al molar fraction increased. For the same Al content, the chemical potential of Al

decreased with the reduction of Ti molar fraction. Therefore, low Al and high Ti content promoted the diffusion of Al atom from molten to the liquid/solid interface and Ti substrate [29]. The Al atom in the Ti substrate and solid/liquid interface was saturated inducing the precipitation of  $\text{Al}_3\text{Ti}$  phase indicated in Figure 14c. When the temperature decreased to 325 °C, the eutectic reaction occurred with  $\alpha\text{-Mg} + \text{Mg}_{17}\text{Al}_{12}$  [30], as shown in Figure 14d. As a result, the couple could form a complete metallurgical bonding formed at the Mg-9Al/Ti interface.

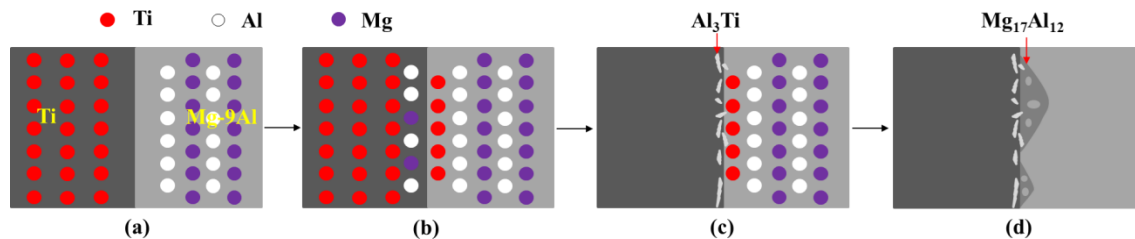


**Figure 14.** Schematic diagram of the metallurgical reaction mechanism of the solid/liquid interface. (a,b) diffusion of Ti atoms and Al atoms at the interface, (c) precipitation of  $\text{Al}_3\text{Ti}$  phase in the Ti substrate and solid/liquid interface, (d) solidification of interfacial zone.

#### 4. Conclusions

In this paper, the effects of different heat treatment time on the microstructures, mechanical properties, and fractographies of the Mg-9Al/Ti metallurgical bonding by liquid-solid diffusion couples were investigated. The obtained results can be summarized as follows.

- (1) The  $\text{Mg}_{17}\text{Al}_{12}$  in the Mg-9Al matrices was attached to the surface of Ti rods. Grain boundaries Ti and Mg-9Al wetting transition from incompletely wetted to completely wetted by  $\text{Mg}_{17}\text{Al}_{12}$  phase. A metallurgical bond was established at the interface between Mg-9Al alloy and Ti matrices. The impurity diffusion coefficients of Mg in Ti and Al in Ti, and Ti in Mg-9Al are  $1.70(\pm 0.02) \times 10^{-15} \text{ m}^2/\text{s}$ ,  $3.77(\pm 0.12) \times 10^{-15} \text{ m}^2/\text{s}$ ,  $1.60(\pm 0.23) \times 10^{-14} \text{ m}^2/\text{s}$ , respectively. The diffusion of Al and Ti elements play an important role during the interface of Mg-9Al/Ti metallurgical bonding.
- (2) Shear strength of Mg-9Al/Ti metallurgical bonding was presented an increasing tendency in perfect accordance with heat treatment time. Shear strength could reach the maximum value of 56 MPa. The fracture was took place along Mg-9Al matrix at the interface. Shear stress greatly improves when Al and Ti interdiffused and chemical interaction occurs between Mg-9Al and Ti.
- (3) By EDS and XRD analysis, these results were found that  $\text{Al}_3\text{Ti}$  is the only intermetallic compound at the interface of the Mg-9Al/Ti compound castings. Gibbs free energies of formation of  $\text{AlTi}_3$ ,  $\text{AlTi}$ ,  $\text{Al}_3\text{Ti}$ ,  $\text{Al}_2\text{Ti}$  and  $\text{Al}_5\text{Ti}_2$  were calculated. The result was shown that  $\text{Al}_3\text{Ti}$  is expected to be the first phase to form in the Al-Ti system.

**Author Contributions:** B.J., C.P. and F.P. designed the project and guided the research. J.D, Z.J., Q.Y. (Qingshan Yang) and Q.C. performed the experiment and analyzed the data. Q.Y. (Qiong Yan). and H.X. investigated the project. J.D. wrote and reviewed the manuscript.

**Funding:** This research was funded by the Chongqing Science and Technology Commission (Grant No. cstc2017cyjAX0394), the Scientific and Technological Research Program of Chongqing Municipal Education Commission (Grant No. KJ1712301), the Fuling Science and Technology Commission (Grant No. FLKW, 2017ABA1014), the Fundamental Research Funds for the Yangtze Normal University (Grant No. 2016KYQD15), the National Natural Science Foundation of China (Grant No. 51701033), the Talent project of Chongqing University of Arts and Sciences (Grant No. 2017RXC24), the undergraduate research project for the Yangtze Normal University.

**Acknowledgments:** The authors thank Jianyue Zhang (Purdue University) for the language improvement.

**Conflicts of Interest:** The authors declare no conflict of interest.

## References

1. Wang, X.J.; Xu, D.K.; Wu, R.Z.; Chen, X.B.; Peng, Q.M.; Jin, L.; Xin, Y.C.; Zhang, Z.Q.; Liu, Y.; Chen, X.H. What is going on in magnesium alloys? *J. Mater. Sci. Technol.* **2017**, *34*, 245–247. [[CrossRef](#)]
2. Pan, H.; Ren, Y.; Fu, H.; Zhao, H.; Wang, L.; Meng, X.; Qin, G. Recent developments in rare-earth free wrought magnesium alloys having high strength: A review. *J. Alloys Compd.* **2015**, *663*, 321–331. [[CrossRef](#)]
3. Pan, F.; Chen, X.; Yan, T.; Liu, T.; Mao, J.; Luo, W.; Wang, Q.; Peng, J.; Tang, A.; Jiang, B. A novel approach to melt purification of magnesium alloys. *J. Magnes. Alloys* **2016**, *4*, 8–14. [[CrossRef](#)]
4. Gorynin, I.V. Titanium alloys for marine application. *Mater. Sci. Eng. A* **1999**, *263*, 112–116. [[CrossRef](#)]
5. Ren, Y.M.; Lin, X.; Fu, X.; Tan, H.; Chen, J.; Huang, W.D. Microstructure and deformation behavior of Ti-6Al-4V alloy by high-power laser solid forming. *Acta Mater.* **2017**, *132*, 82–95. [[CrossRef](#)]
6. Neugebauer, J. Theory-guided bottom-up design of beta-titanium alloys as biomaterials based on first principles calculations: Theory and experiments. *Acta Mater.* **2007**, *55*, 4475–4487.
7. Chen, M.C.; Hsieh, H.C.; Wu, W. The evolution of microstructures and mechanical properties during accumulative roll bonding of Al/Mg composite. *J. Alloys Compd.* **2006**, *416*, 169–172. [[CrossRef](#)]
8. Feng, B.; Xin, Y.; Guo, F.; Yu, H.; Wu, Y.; Liu, Q. Compressive mechanical behavior of Al/Mg composite rods with different types of Al sleeve. *Acta Mater.* **2016**, *120*, 379–390. [[CrossRef](#)]
9. Gao, M.; Mei, S.; Li, X.; Zeng, X. Characterization and formation mechanism of laser-welded Mg and Al alloys using Ti interlayer. *Scripta Mater.* **2012**, *67*, 193–196. [[CrossRef](#)]
10. Jiang, W.; Li, G.; Fan, Z.; Wang, L.; Liu, F. Investigation on the Interface Characteristics of Al/Mg Bimetallic Castings Processed by Lost Foam Casting. *Metall. Mater. Trans. A* **2016**, *47*, 2462–2470. [[CrossRef](#)]
11. Zhao, K.N.; Liu, J.C.; Nie, X.Y.; Li, Y.; Li, H.X.; Du, Q.; Zhuang, L.Z.; Zhang, J.S. Interface formation in magnesium–magnesium bimetal composites fabricated by insert molding method. *Mater. Des.* **2016**, *91*, 122–131. [[CrossRef](#)]
12. Nie, X.Y.; Liu, J.C.; Li, H.X.; Du, Q.; Zhang, J.S.; Zhuang, L.Z. An investigation on bonding mechanism and mechanical properties of Al/Ti compound materials prepared by insert moulding. *Mater. Des.* **2014**, *63*, 142–150. [[CrossRef](#)]
13. Predel, B. *Mg-Ti (Magnesium-Titanium)*; Springer: Berlin, Germany, 1997.
14. Cao, R.; Wang, T.; Wang, C.; Feng, Z.; Lin, Q.; Chen, J.H. Cold metal transfer welding–brazing of pure titanium TA2 to magnesium alloy AZ31B. *J. Alloys Compd.* **2014**, *605*, 12–20. [[CrossRef](#)]
15. Tan, C.; Chen, B.; Meng, S.; Zhang, K.; Song, X.; Zhou, L.; Feng, J. Microstructure and mechanical properties of laser welded-brazed Mg/Ti joints with AZ91 Mg based filler. *Mater. Des.* **2016**, *99*, 127–134. [[CrossRef](#)]
16. Tan, C.; Song, X.; Chen, B.; Li, L.; Feng, J. Enhanced interfacial reaction and mechanical properties of laser welded-brazed Mg/Ti joints with Al element from filler. *Mater. Lett.* **2016**, *167*, 38–42. [[CrossRef](#)]
17. Straumal, B.B.; Gornakova, A.S.; Kogtenkova, O.A.; Protasova, S.G.; Sursaeva, V.G.; Baretzky, B. Continuous and discontinuous grain-boundary wetting in  $Zn_xAl_{1-x}$ . *Phys. Rev. B* **2008**, *78*, 054202. [[CrossRef](#)]
18. Protasova, S.G.; Kogtenkova, O.A.; Straumal, B.B.; Baretzky, B. Inversed solid-phase grain boundary wetting in the Al–Zn system. *J. Mater. Sci.* **2011**, *46*, 4349–4353. [[CrossRef](#)]
19. Jie, W.Q.; Kandalova, E.G.; Zhang, R.J. Al<sub>3</sub>Ti/Al composites prepared by SHS. *Rare Metal Mat. Eng.* **2000**, *29*, 145–148.
20. Palm, M.; Zhang, L.C.; Stein, F.; Sauthoff, G. Phases and phase equilibria in the Al-rich part of the Al–Ti system above 900 °C. *Intermetallics* **2002**, *10*, 523–540. [[CrossRef](#)]
21. Paul, W.; Oliver, D.; Miyahara, Y.; Grutter, P. Transient adhesion and conductance phenomena in initial nanoscale mechanical contacts between dissimilar metals. *Nanotechnology* **2013**, *24*, 475704. [[CrossRef](#)] [[PubMed](#)]
22. Dutheil, P.; Thomann, A.L.; Lecas, T.; Brault, P.; Vayer, M. Sputtered Ag thin films with modified morphologies: Influence on wetting property. *Appl. Surf. Sci.* **2015**, *347*, 101–108. [[CrossRef](#)]
23. Torrisi, V.; Ruffino, F. Nanoscale structure of submicron-thick sputter-deposited Pd films: Effect of the adatoms diffusivity by the film-substrate interaction. *Surf. Coat. Tech.* **2017**, *315*, 123–129. [[CrossRef](#)]
24. Sarafianos, N. An analytical method of calculating variable diffusion coefficients. *J. Mater. Sci.* **1986**, *21*, 2283–2288. [[CrossRef](#)]
25. Rawers, J.C.; Wrzesinski, W.R. Reaction-sintered hot-pressed TiAl. *J. Mater. Sci.* **1992**, *27*, 2877–2886. [[CrossRef](#)]

26. Abboud, J.H.; West, D.R.F. Microstructures of titanium-aluminides produced by laser surface alloying. *J. Mater. Sci.* **1992**, *27*, 4201–4207. [[CrossRef](#)]
27. Sujata, M.; Bhargava, S.; Sangal, S. On the formation of  $TiAl_3$  during reaction between solid Ti and liquid Al. *J. Mater. Sci. Lett.* **1997**, *16*, 1175–1178. [[CrossRef](#)]
28. Kattner, U.R.; Lin, J.C.; Chang, Y.A. Thermodynamic assessment and calculation of the Ti-Al System. *Metall. Trans. A* **1992**, *23*, 2081–2090. [[CrossRef](#)]
29. Chen, S.H.; Li, L.Q.; Chen, Y.B.; Liu, D.J. Si diffusion behavior during laser welding-brazing of Al alloy and Ti alloy with Al-12Si filler wire. *T. Nonferr. Metal. Soc.* **2010**, *20*, 64–70. [[CrossRef](#)]
30. Zhang, J.; Guo, Z.X.; Pan, F.; Li, Z.; Luo, X. Effect of composition on the microstructure and mechanical properties of Mg–Zn–Al alloys. *Mater. Sci. Eng. A* **2007**, *456*, 43–51. [[CrossRef](#)]



© 2018 by the authors. Licensee MDPI, Basel, Switzerland. This article is an open access article distributed under the terms and conditions of the Creative Commons Attribution (CC BY) license (<http://creativecommons.org/licenses/by/4.0/>).